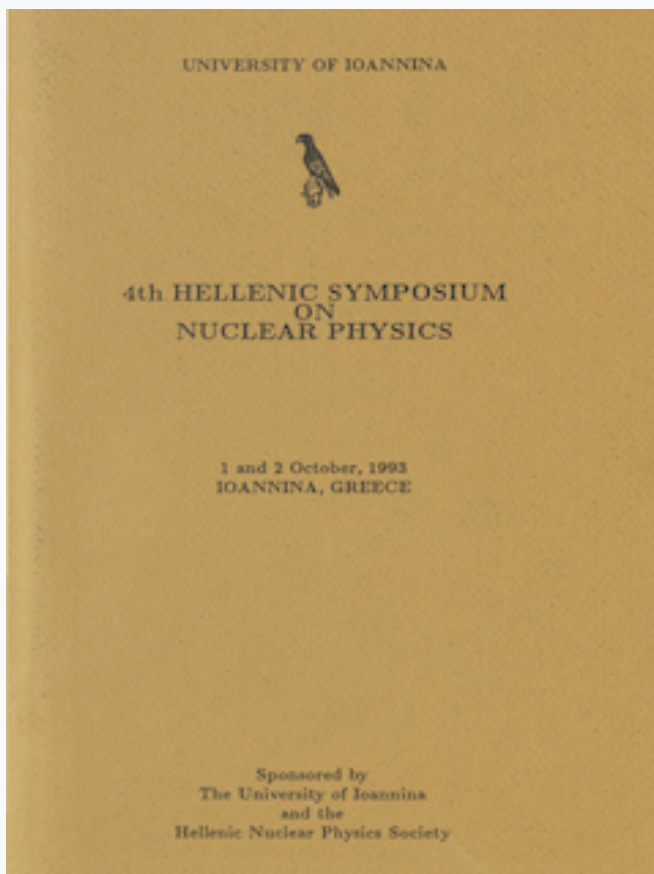


## HNPS Advances in Nuclear Physics

Vol 4 (1993)

HNPS1993



### On some interesting aspects of heavy-ion reactions studied with $7\text{Li}+11\text{B}$ and $9\text{Be}+9\text{Be}$

*E. Adamides, C. T. Papadopoulos, R. Vlastou, E. N. Gazis, A. A. Pakou, P. A. Assimakopoulos, G. Doukelis, C. A. Kalfas, A. C. Xenoulis*

doi: [10.12681/hnps.2871](https://doi.org/10.12681/hnps.2871)

### To cite this article:

Adamides, E., Papadopoulos, C. T., Vlastou, R., Gazis, E. N., Pakou, A. A., Assimakopoulos, P. A., Doukelis, G., Kalfas, C. A., & Xenoulis, A. C. (2020). On some interesting aspects of heavy-ion reactions studied with  $7\text{Li}+11\text{B}$  and  $9\text{Be}+9\text{Be}$ . *HNPS Advances in Nuclear Physics*, 4, 21–25. <https://doi.org/10.12681/hnps.2871>

## On some interesting aspects of heavy ion reactions

studied with  ${}^7\text{Li}+{}^{11}\text{B}$  and  ${}^9\text{Be}+{}^9\text{Be}$ 

E. Adamides, C. T. Papadopoulos, R. Vlastou and E. N. Gazis  
National Technical University of Athens, Phys. Dept. Athens, Greece  
A. A. Pakou and P. A. Assimakopoulos  
University of Ioannina, Phys. Dept., Ioannina, Greece  
G. Doukelis, C. A. Kalfas and A. C. Xenoulis  
Institute of Nuclear Physics, NCSR " Demokritos " GR 153 10, Greece

## I. Introduction

Among the interesting aspects which concern the mechanism of heavy ion reactions are the following two:

1) The deformation brought into the compound nucleus by the fused heavy ion system and how this phenomenon influences the subsequent decay of the compound nucleus<sup>1,2</sup>. This deformation would cause a reduction of the barrier height seen by the various particles evaporated from the compound system which would change in many cases their competition.

2) Particularly in light heavy ion reactions involving loosely bound nuclei the total fusion cross section was found to be only a small part of the reaction cross section even at low energies where one would expect the compound nucleus to be the dominant reaction mechanism<sup>3,4</sup>. This phenomenon could be attributed to the high probability for break up of the weakly bound nuclei before complete fusion is reached or alternatively to the existence of a limiting angular momentum in the framework of the compound nucleus.

In the present work we mainly studied the above phenomena in the reactions  ${}^7\text{Li}+{}^{11}\text{B}$  and  ${}^9\text{Be}+{}^9\text{Be}$  through measurements of the  $\gamma$  ray cross sections of the residual nuclei produced. These reactions form the same compound nucleus  ${}^{18}\text{O}$  at similar excitation energies and angular momenta and thus their parallel study helps to separate the contribution of compound and non compound processes which coexist in several exit channels and which otherwise would cause difficulties to our study.

## II. Experimental procedure and analysis

The measurements have been performed using the  ${}^7\text{Li}$  and  ${}^9\text{Be}$  beams of the T11/25 Tandem Van de Graaf accelerator of the National Research Center "Demokritos". The  ${}^{11}\text{B}$  and  ${}^9\text{Be}$  targets were composed respectively of 323 and 105  $\mu\text{g}/\text{cm}^2$  layers of enriched  ${}^{11}\text{B}$  and  ${}^9\text{Be}$  isotopes evaporated onto 100  $\text{mg}/\text{cm}^2$  of Ta and Au backing. The backing ensured complete stopping in the target and was used both to monitor the beam current and to reduce the large  $\gamma$ -ray Doppler broadening. The targets were placed in a 10 cm diameter cylindrical scattering chamber with a cold trap on top to keep the inside walls at liquid nitrogen temperature to avoid carbon build up on the target.

The beam entered the chamber through a 30 cm long tube insulator from the rest of the beam line. This geometry helped the measurement of the beam current by collecting the charge from the whole arrangement ( target, cham-

ber and tube ). For an accurate measurement of the integrated beam charge the experimental coulomb excitation cross sections for the 301 KeV Ta and the 279 KeV Au  $\gamma$ -rays were calculated according to the thick-target semi-classical theory of Alder et al<sup>5</sup>. The  $\gamma$ -ray branching ratios of the 301 and 279 KeV states to the ground state in Ta and Au respectively as well as the B(E2) strength and internal conversion coefficients used in the calculations were taken from refs. 5 and 6.

Singles  $\gamma$  ray spectra were obtained with a 95 cm<sup>3</sup> Ge(Li) detector at an angle of 125° and a HpGe detector at 55° with respect to the beam direction. One detector was used to get the detailed low energy  $\gamma$ -ray spectra and the other to get all  $\gamma$  rays up to 7 MeV. Since the second order polynomial P<sub>2</sub> almost vanishes at 55° and 125° these spectra were taken to represent angle integrated yields. In addition the considerable Doppler broadening and shift at these angles allowed simple identification of  $\gamma$  rays in conjunction with some low and high energy spectra taken at 90°.

Both detectors were placed at a distance of 12 cm from the target and were lead shielded to avoid beam tube background and to suppress low energy  $\gamma$  rays. The relative efficiencies curve of the two detectors were determined from <sup>56</sup>Co and <sup>152</sup>Eu spectra under the conditions of the experiments and in the same way the absolute efficiencies by using a standard calibrated <sup>60</sup>Co source.

The singles  $\gamma$ -ray spectra were taken in the range of 5.0 - 19.0 MeV incident <sup>9</sup>Be energy and in the range of 5.5 - 19.0 MeV incident <sup>7</sup>Li energy in approximately 0.5 MeV steps. Initial measurements were repeated every six hours during the experiment and in the end to check for carbon build up and oxygen contamination. Characteristic  $\gamma$ -rays coming from the reactions with the carbon and oxygen were used to monitor these contaminants and have a good estimation of their contributions to the  $\gamma$ -ray spectra; these contributions were found to be negligible.

The  $\gamma$ -ray cross sections for the various transitions in the residual nuclei were obtained as:

$$\sigma_{\gamma} = N_{\gamma} / \epsilon_{\gamma} N_{\beta} N_{T}$$

where:

$N_{\gamma}$  is the number of counts in the  $\gamma$ -ray peak.

$\epsilon_{\gamma}$  the corresponding detection efficiency for the  $\gamma$ -ray. Knowledge of all three efficiencies ( full energy, first and second escape ) facilitated also the analysis of multiple peaks.

$N_{\beta}$  the number of incident beam particles. As was stated in section II  $N_{\beta}$  was found from the beam current integrator system mainly at the lower incident energies as well as the Coulomb excitation of the Ta or Au backing. mainly at the higher incident energies. Unlike the normalization by current integration the normalization by Coulomb excitation can correct for the dead time of the acquisition system which was sometimes appreciable at the higher bombarding energies used. When both methods were applied they gave the same results.

$N_{T}$  the number of target nuclei per cm<sup>2</sup> calculated from the surface density of the target .

The overall error in the evaluation of the  $\gamma$ -ray cross section due to uncertainties in  $\epsilon_{\gamma}$ ,  $N_{\gamma}$  and  $N_{T}$  was around 10%.

### III. Results and discussion

Cross sections for  $\gamma$  rays were obtained versus incident energy (from little below to around three times the Coulomb barrier) for the following exit channels:  $p+^{17}\text{N}$ ,  $n+^{17}\text{O}$ ,  $t+^{15}\text{N}$ ,  $\alpha+^{14}\text{C}$ ,  $pn+^{16}\text{N}$ ,  $nn+^{16}\text{O}$ ,  $an+^{13}\text{C}$ ,  $\alpha\alpha+^{10}\text{Be}$ , and  $d2n+^{12}\text{C}$ . As examples the cross sections for the 6728 KeV - 0  $\gamma$ -ray transition of the  $\alpha$ /tp emission channel from both reactions  $^7\text{Li}+^{11}\text{B}$  and  $^9\text{Be}+^9\text{Be}$  are shown versus c.m. energy in Fig. 1 and that for the  $\gamma$ -ray transition 3854 KeV - 0 of the  $^{13}\text{C}$  exit channel from the  $^9\text{Be}+^9\text{Be}$  reaction in Fig. 2. Our measurements were performed under better conditions ( finer energy resolution and less Doppler broadening ) and wider energy range compared to ref. 7.

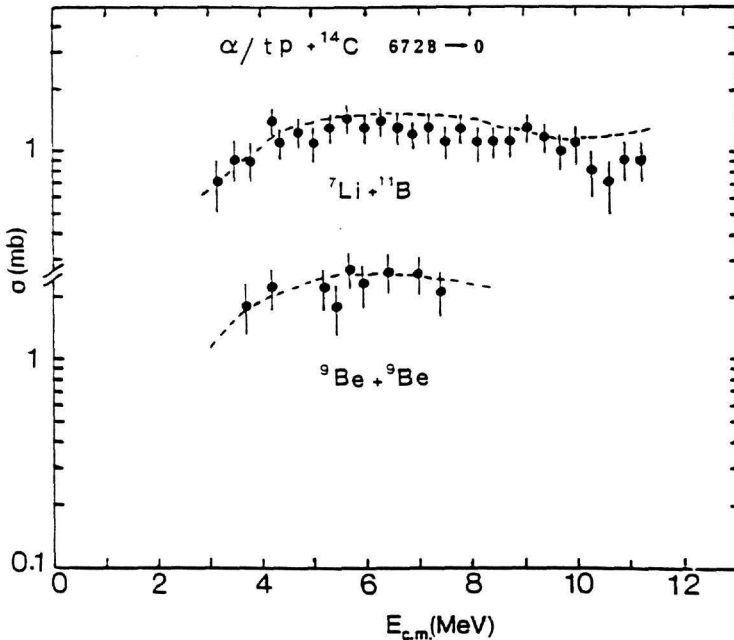


Fig. 1. Excitation function for the 6728 KeV transition of  $^{14}\text{C}$  produced by the  $^7\text{Li}+^{11}\text{B}$  and  $^9\text{Be}+^9\text{Be}$  reactions. The dashed lines are the corresponding theoretical predictions from statistical model calculations using the code STAPRE.

From the excitation functions one can observe that most of the curves have the bell shape characteristic of both the compound and transfer processes. The curves for the  $\alpha+^{14}\text{C}$  ( see Fig.1 ) and  $t+^{15}\text{N}$  channels after a small drop go up again because of contributions from multiparticle processes. The cross section for the  $nn+^{12}\text{C}$  4.439 MeV - 0  $\gamma$  transition is still increasing at the higher incident energies where according to the statistical evaporation model is more favourable.

In order to investigate the mechanism of the reactions  $^9\text{Be}+^9\text{Be}$  and  $^7\text{Li}+^{11}\text{B}$  we have performed theoretical calculations of the cross sections for the various transitions in the produced residual nuclei in the framework of the Hauser-Feshbach theory for compound nucleus reactions using the code STAPRE<sup>8</sup> and the DWBA method using the code DWUCK4<sup>9</sup> for the channels where the transfer process is important i.e.  $^{11}\text{B}(^7\text{Li},t)^{15}\text{N}$ ,  $^9\text{Be}(^9\text{Be},an)^{13}\text{C}$  and

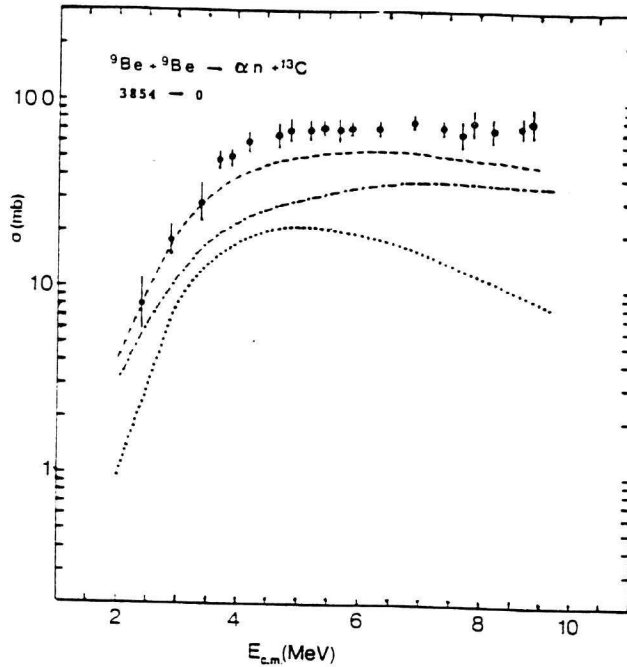


Fig. 2. Excitation function for the  $^{13}\text{C}$ , 3854 KeV  $\gamma$  ray in the  $\alpha$ -transfer channel. The various lines represent theoretical predictions from statistical model calculations (dotted-dashed line), from DWBA calculations (dotted line) and both statistical and DWBA calculations (dashed line) normalized to the data at low energies.

$^9\text{Be}(^9\text{Be}, 2\alpha)^{10}\text{Be}$ . We have considered the p and n channels as being formed by the compound nucleus procedure and we fixed the parameters  $a$ ,  $r_B$  and  $V_B$  entering the code STAPRE for a best fit to the  $\gamma$  ray cross section curves of these channels.

A comparison of the theoretical calculations with experimental results reveals the following:

Theory based on the compound nucleus statistical model (without the inclusion of deformation) agrees with the experimental  $\gamma$  ray cross section curves for the one particle emission channels i.e. p, n,  $\alpha$ . It is impressive to notice in the case of  $\alpha$ /tp emission channel (Fig. 1) that Hauser-Feshbach theory can predict the increase at higher energies of the cross section due to the opening of the tp multiparticle channel.

On the contrary theory disagrees with experiment in most cases of the two particle emission channels (nn, np, an and  $\alpha\alpha$ ) even if transfer contributions were taken into account (see Fig. 2). Specifically theory underpredicts the  $\gamma$  ray cross sections in the np, an and  $2\alpha$  emission channels while it overpredicts the nn.

The above discrepancies can be raised if deformation is included into the statistical compound nucleus calculations. Deformation in the compound nucleus causes a reduction of the barrier height for the various emitted particles (i.e. it affects their transmission coefficients) and can alter in many cases the production cross section in the exit channels. Specifically: The theoretical  $\gamma$  ray cross section curves remain unchanged for the

one particle emission channels which are produced mainly by side feeding from the tail of the particle emission spectra. On the contrary for the two particle emission channels observable alterations do occur. The theoretical  $\gamma$  ray cross sections in the case of the np,  $\alpha n$  and  $2\alpha$  emission channels are increased because they are produced by side feeding from the very low energy part of the particle emission spectra and which is favoured by the reduction of the barrier for protons and alphas while they are decreased in the case of the nn emission channel where sizeable feeding from above exists and which is reduced when deformation is included.

Regarding the total fusion cross section we found it to be much less than the reaction cross section for both reactions and for the whole energy region studied in accordance with previous results<sup>3,4</sup>

### References

- [1]. R. Lacey, N. N. Ajitanand, J. M. Alexander et al, Phys. Rev. C37, 2561 (1988).
- [2]. N. G. Nicolis, D. G. Sarantites, L. A. Adler et al, Phys. Rev. C41, 2118 (1990).
- [3]. L.Fante Jr., N. Added, R. M. Anjos et al, Nucl. Phys. A552, 82 (1993).
- [4]. J. F. Mateja, J. Garman, D. E. Fields et al, Phys. Rev. C30, 134 (1984).
- [5]. K. Alder, A. Bohr, T. Huus et al, Rev. Mod. Phys. 28, 432 (1956 ).
- [6]. P. R. Sharma, Nucl. Phys. A154, 312 (1970).
- [7]. B. Dasmahapatra, B. Cujec, G. Kajrys et al, Nucl. Phys. A564, 314 (1993).
- [8]. Program STAPRE, M. Uhl., Acta Phys. Austriaca 31, 245 (1970).
- [9]. Program DWUCK4, P. D. Kunz ( unpublished ); Extended version of J. R. Confort ( unpublished ).